PNAS
www.pnas.org

Supplementary Materials for

Phosphorylation-guarded light-harvesting complex II contributes to broad-spectrum blast resistance in rice

Muxing Liu[a,b], Suobing Zhang[c], Jiexiong Hu[a,b], Wenxian Sun[d], Jonas Padilla[c], Yanglan He[a,b], Ying Li[a,b], Ziyi Yin[a,b], Xinyu Liu[a,b], Wenhao Wang[a,b], Danyu Shen[a,b], Dayong Li[d], Haifeng Zhang[a,b], Xiaobo Zheng[a,b], Zhongli Cui[e], Guo-Liang Wang[f], Ping Wang[g,h], Bo Zhou[c,i], and Zhengguang Zhang[a,b,1]

*Corresponding author. Email: zhgzhang@njau.edu.cn

This PDF file includes:

Materials and Methods
Figs. S1 to S25
Tables S1 and S2
Captions for Datasets S1 to S3

Other Supplementary Materials for this manuscript include the following:

Datasets S1 to S3

www.pnas.org/cgi/doi/10.1073/pnas.1905123116

Materials and Methods

1. Plant strains

The R4D rice varieties were obtained from Bo Zhou's lab from the International Rice Research Institute. The 15189, 15193, 15194, 15206, 15209, 15213, 15220, 15227, 15236, 15237, NG 23, YLY 4, LG 8, ZD 14, HD 16, HD 21, YD 14, YD 20, WY 13 and JSNJ 1-35 rice varieties were collected in Nanjing, Jiangsu, China. Lijiangxintuanheigu (LTH), and Yangeng456 (YG456) were obtained from the Saline-Alkali Land Utilization and Research Institute, Liaoning, China. The F2 generation was obtained from Wenxian Sun's lab in Jilin Agricultural University. *Oryza sativa japonica* cv. TP309 was transformed with constructs pUCC-LHCB5-RNAi and pCAM2300-LHCB5 with *Agrobacterium* tumefaciens-mediated transformation at Wuhan BIORUN Co., Ltd (Wuhan, China). The plants were grown in the greenhouse or fields at Nanjing Agricultural University in Nanjing, China.

2. *Magnaporthe oryzae* isolates

M. oryzae isolates, Guy11, 51 #, 98-06, 98-21-1, 98-24-1, 98-55-1, 98-83-1, 98-84-1, 98-93-1, 99-21, 99-27, 99-46, 99-66-1, 99-106-2, JS001-19, JS001-32, JS001-33, 2002-10-2, 8036-2, 9403-3, 2013-19 and 2013-46 were used for inoculation. All isolates were cultured in complete medium (CM) in a growth chamber at 28°C. The Mo15-125 and Mo15-19 were obtained from Bo Zhou's lab from the International Rice Research Institute.

3. Resistance test and infection assays

For resistance tests, conidia were suspended to a concentration of 5×10^4 spores per milliliter in 0.2% (w/v) gelatin solution. 5 ml of suspension was sprayed on two-week-old rice seedlings. Inoculated plants were kept in a growth chamber at 25°C with 90% humidity and in the dark for the first 24 hours, followed by a 16/8 hour light/dark cycle. The disease severity was assessed at 7 days after inoculation (41). For observation of the penetration and invasive growth in rice cells, conidial suspensions (1×10^5 spores per milliliter) were injected into leaf sheath. At 28˚C for 24 or 48 hours, the inner epidermises of infected sheaths were observed under a microscope.

4. RNA isolation and qRT-PCR

RNA isolation was performed by TRIzol (Invitrogen Life Technologies, Shanghai, China). cDNA synthesis was performed by PrimeScriptTM RT Reagent Kit (TaKaRa). Quantitative RT-PCR was performed with the ABI 7500 Fast Real-Time System and transcripts were analyzed by the 7500 System SDS software. To compare the relative abundance of target gene transcripts in different rice varieties, the average threshold cycle (Ct) was normalized to rice actin for each of the treated samples as $2^{-\Delta Ct}$, where $-\Delta Ct$= (Ct, target gene-Ct, actin). Fold changes during different rice varieties calculated as $2^{-\Delta\Delta Ct}$, $-\Delta\Delta Ct$= (Ct, experiment-Ct, actin) - (Ct, control-Ct, actin).

5. ROS and cell death observation

To observe ROS derived from rice, we stained rice leaves or sheaths with DAB (Sigma-Aldrich) as described previously (19). For the measurement of ROS levels, the leaves were cut into discs with a cork borer and pre-incubated overnight in sterile-distilled water. After the leaf disks or the isolated protoplast were treated with purified mycelia as elicitors, ROS production was monitored by the luminol chemiluminescence assay (42). Each treatment was represented by

three duplicates. In vivo $O_2^{\bullet-}$ production was monitored by nitroblue tetrazolium (NBT) staining as described previously (43). For cell death observation, we stained the rice leaves or sheaths with trypan blue and then destained with lactophenol prior to the microscopic examination as described previously (44). CAG (catalase of *Aspergillus niger*) and GSH (reduced glutathione) treatments were reported previously (45).

6. Phosphorylation assays

Total proteins from wild type and transgenic rice plants were extracted. Briefly, leaves of rice were ground into powder in liquid nitrogen and resuspended in 1 ml of extraction buffer (10 mM Tris-HCl [pH 7.5], 150 mM NaCl, 0.5 mM EDTA, 0.5% NP40) to which 1mM PMSF, 10 μl of protease inhibitor cocktail (Sigma), and 10 μl of phosphatase inhibitor cocktail 3 (Sigma) were added. The samples were resolved on 10% SDS-polyacrylamide gels prepared with 50 μM acrylamide-pendant Phos-tag ligand and 100 μM $MnCl_2$ according to the instructions provided by the Phos-tag Consortium. Gels were electrophoresed at 80 V/gel for 3-6 h. Prior to the transfer, gels were first equilibrated in transfer buffer containing 5 mM EDTA for 20 min two times and then in transfer buffer without EDTA for 10 min. Protein transfer from the Mn^{2+}-Phos-tag^{TM} acrylamide gel to the PVDF membrane was performed overnight at 80 V at 4°C, and then the membrane was analyzed by Western blotting (41).

7. In vitro pull-down assay

To construct GST-fusion plasmid, *LHCB5* was inserted into the vector pGEX4T-2 (GE Healthcare Life Science). To construct His-fusion plasmid, PSBS was inserted into the vector pET-32a (Navogen). Pull-down assay was carried out using ProFound pull-down GST protein-protein interaction kit (Pierce) according to the manufacturer's instructions. Briefly, GST or OsLHCB5-GST was expressed in *E. coli* strain BL21 (DE3). Soluble proteins were incubated with 50 μl glutathione agarose beads (Invitrogen) for 1 h at 4˚C. The beads were washed six times and then incubated with an equal amount of bacterial lysates containing PsbS-His for another hour at 4˚C. The beads were washed six times again, and the presence of PsbS-His was detected by immunoblotting using the anti-His antibody (Abmart) (41).

8. Chloroplast isolation

There are two parts to the isolation of chloroplasts. For isolating protoplasts, a razor blade was used to cut the stems and leaves into ~0.5 mm strips. They were then placed into a petri dish containing 10 ml enzyme solution (1.5% cellulase and 0.3% macerozyme). The vacuum was applied for 1 hour for the infiltration of the enzyme solution. Plants were incubated for about 4 hours in the dark with gentle shaking (~ 40 rpm) at room temperature and the solution was removed with a glass pipet. 10 ml W5 medium was added and allowed gently swirl (80 rpm) for 1 hour to release the protoplast. W5 Protoplasts were filtered through a 35 μm nylon mesh, transferred into an 8 ml glass vial, precipitated at 220 g for 4 minutes (46). The isolated chloroplast was used for Western blot analysis with the LHCB1-6 antibody (Agrisera).

9. Statistical analysis

Each experiment was performed at least three replicated measurements and represented as the mean ± standard deviation (SD). The significant differences between treatments were statistically determined by one-way analysis of variance (ANOVA) comparison, and followed by T-test if the ANOVA analysis is significant at $P< 0.05$ or $P< 0.01$.

Figure S1

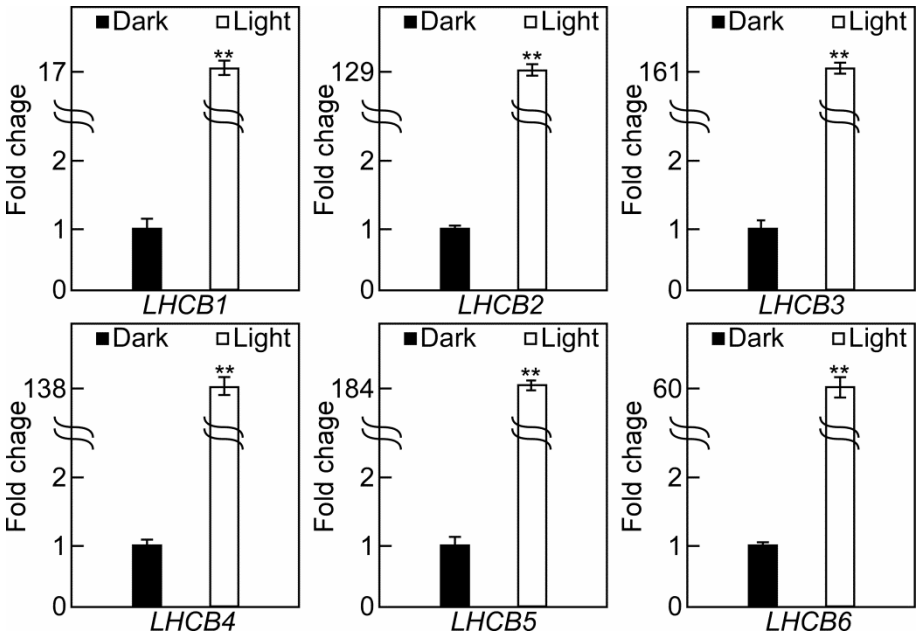

Fig. S1. The expression of *LHCB* genes is regulated by light.

Expression levels of *LHCB* family genes in TP309 treated with the darkness or light were analyzed by qRT-PCR. An asterisk indicates a significant difference between dark and light according to Student's t-test ($P < 0.01$).

Figure S2

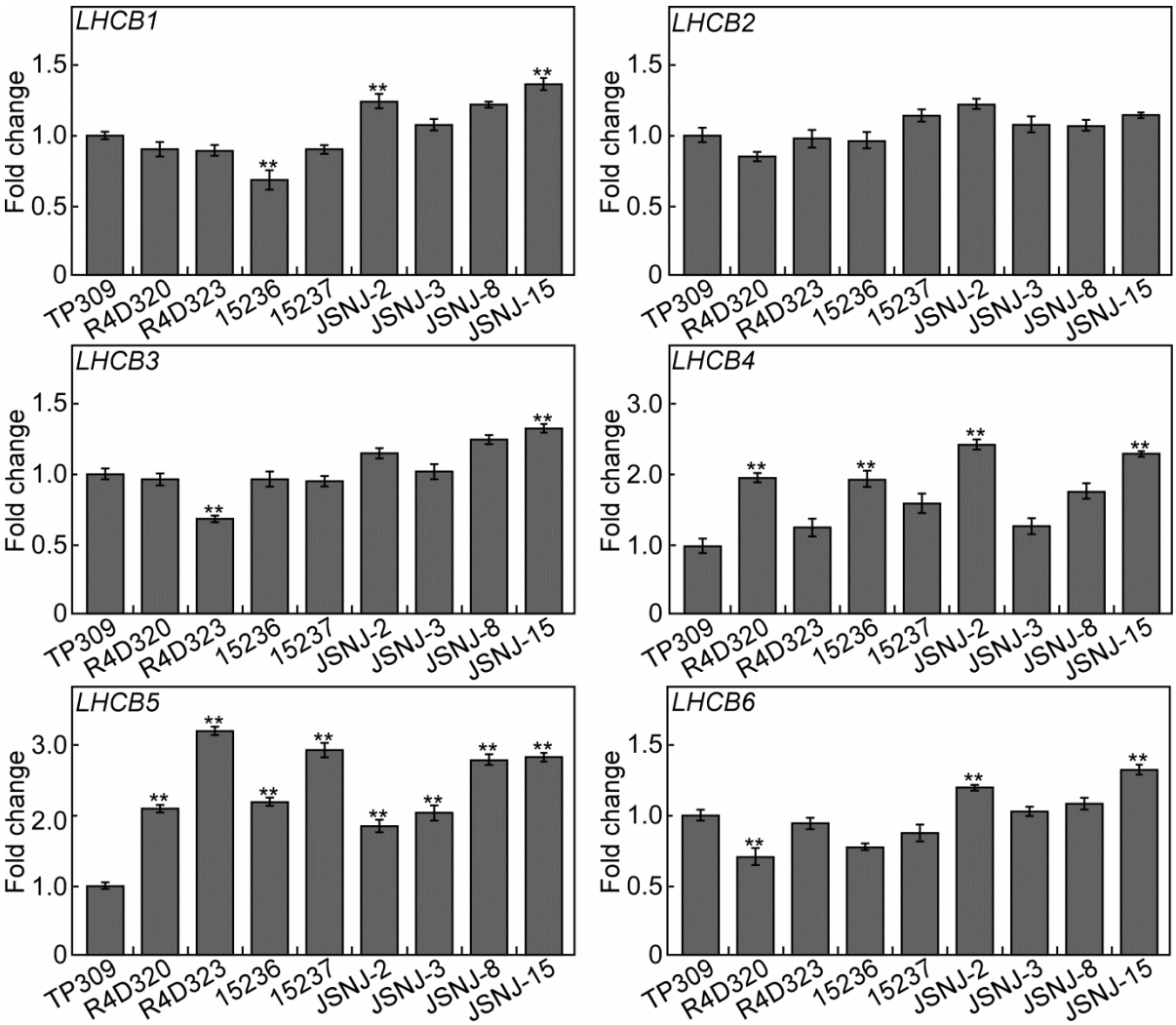

Fig. S2. The expression of *LHCB* genes in eight resistance rice varieties.

Expression levels of *LHCB* family genes in eight resistance rice varieties showed in Figure 1 were analyzed by qRT-PCR. An asterisk indicates a significant difference between TP309 and eight resistance rice varieties according to Student's t test ($P < 0.01$).

Figure S3

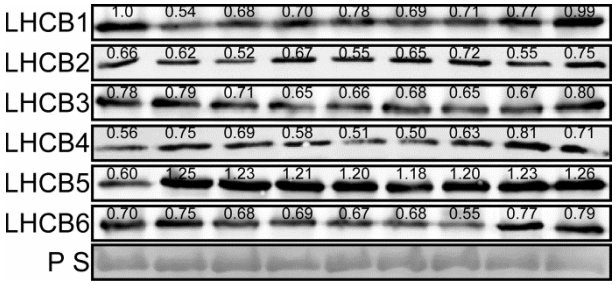

Fig. S3. The protein level of the LHCB family was determined by immunoblotting in the eight resistance rice varieties.

Total protein was extracted from rice seedlings and subjected to SDS-PAGE, followed by immunoblot analysis using anti-LHCB1~6 polyclonal antibodies. The relative band intensity was quantified by ImageJ software. Protein loading is indicated with Ponceau staining (P S).

Figure S4

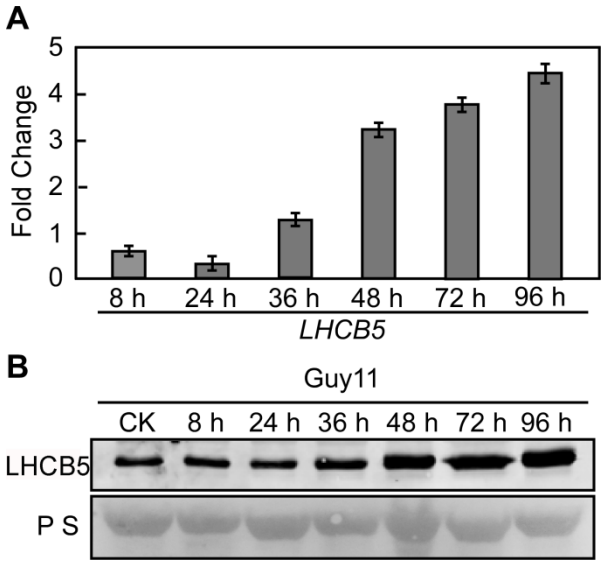

Fig. S4. The transcription and translation of *LHCB5* were induced by the infection of *M. oryzae*.

(A) The transcription of *LHCB5* was induced by the infection of *M. oryzae*. qRT-PCR on *LHCB5* in TP309 at different infectious stages in comparison with non-infected TP309. RNA was extracted from different infectious stages (8, 24, 36, 48, 72 and 96 hpi), respectively. **(B) The translation of *LHCB5* was induced by the infection of *M. oryzae*.** The protein level of LHCB5 in the different infectious stages was determined by immunoblotting using anti-LHCB5 polyclonal antibodies. Protein loading is indicated with Ponceau staining (P S).

Figure S5

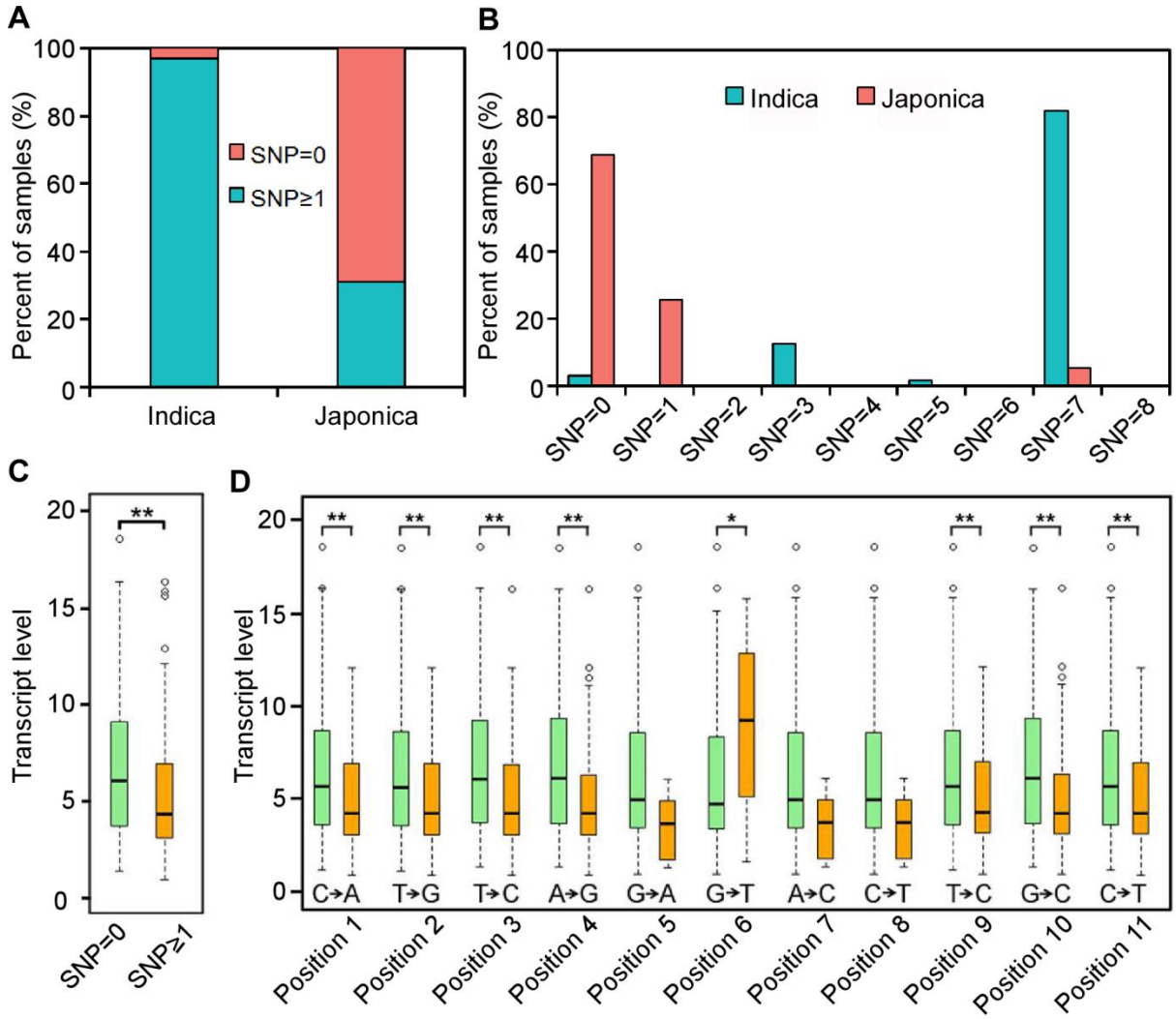

Fig. S5. Identification of SNPs in the *LHCB5* promoter.

(A and B) SNPs distribution in *indica* and *japonica* rice varieties. SNP = 0 indicated the promoter sequence of *LHCB5* was as the same as *Oryza sativa* ssp *japonica* cv. Nipponbare (NPB), which was used as the control. SNP≥1 indicated at least one base change. The promoter sequences of *LHCB5* in 3,000 sequenced rice genomes (Dataset S1) were available in the CNCGB and CAAS database (18). **(C and D) The expression level of *LHCB5* was decreased in SNPs variation rice varieties.** Position 1 to11 indicated the 11 SNPs in different locations of promoter regions. The green boxes indicated the control sequence and the yellow boxes indicated the SNP variation sequence. The expression level of 238 rice varieties (Dataset S3) from 3,000 rice resources was analyzed by qRT-PCR (T-test, **P*<0.05, ***P*<0.01).

Figure S6

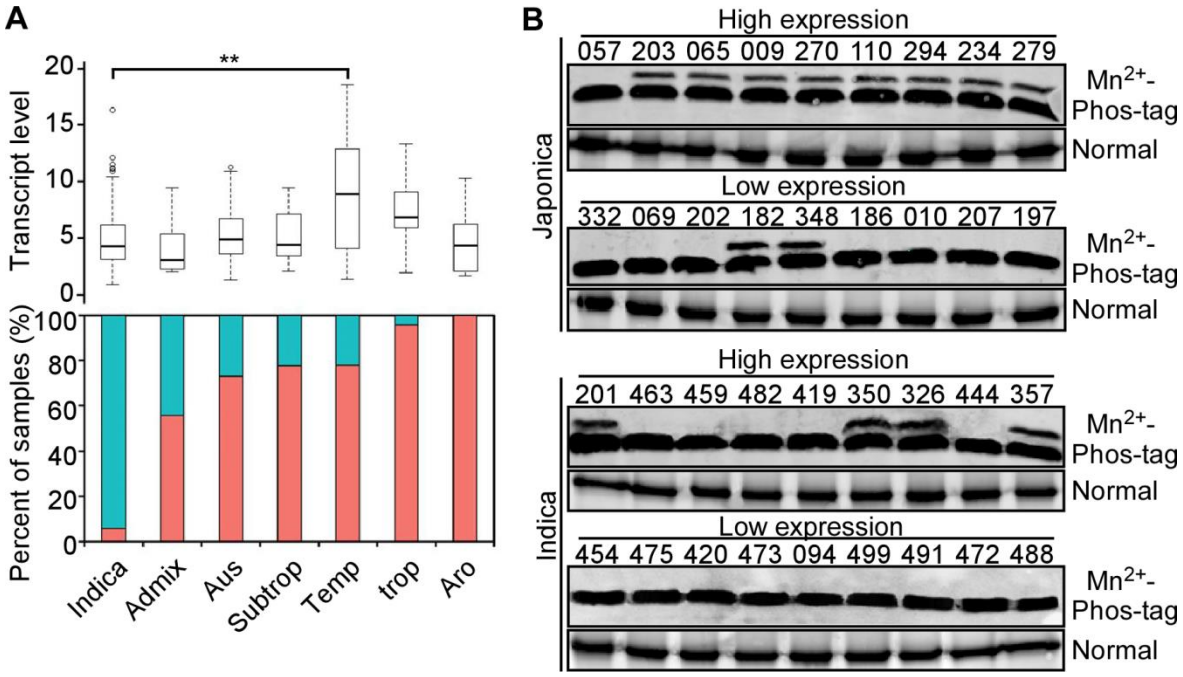

Fig. S6. Differentiation of LHCB5 phosphorylation in *indica* and *japonica*.

(A) The *japonica* rice varieties showed a higher transcript level of *LHCB5* than *indica* varieties. The expression level of 238 rice varieties (Dataset S3) from 3,000 rice resources was analyzed by qRT-PCR (T-test, $^{**}P<0.01$). **(B) LHCB5 was phosphorylated mainly in *japonica* varieties with high expression.** Proteins from *indica* and *japonica* rice leaves inoculate with Guy11 at 2 dpi extracts treated with phosphatase inhibitors were subjected to normal and Phos-tag SDS-PAGE followed by immunoblotting with the LHCB5 polyclonal antibody.

Figure S7

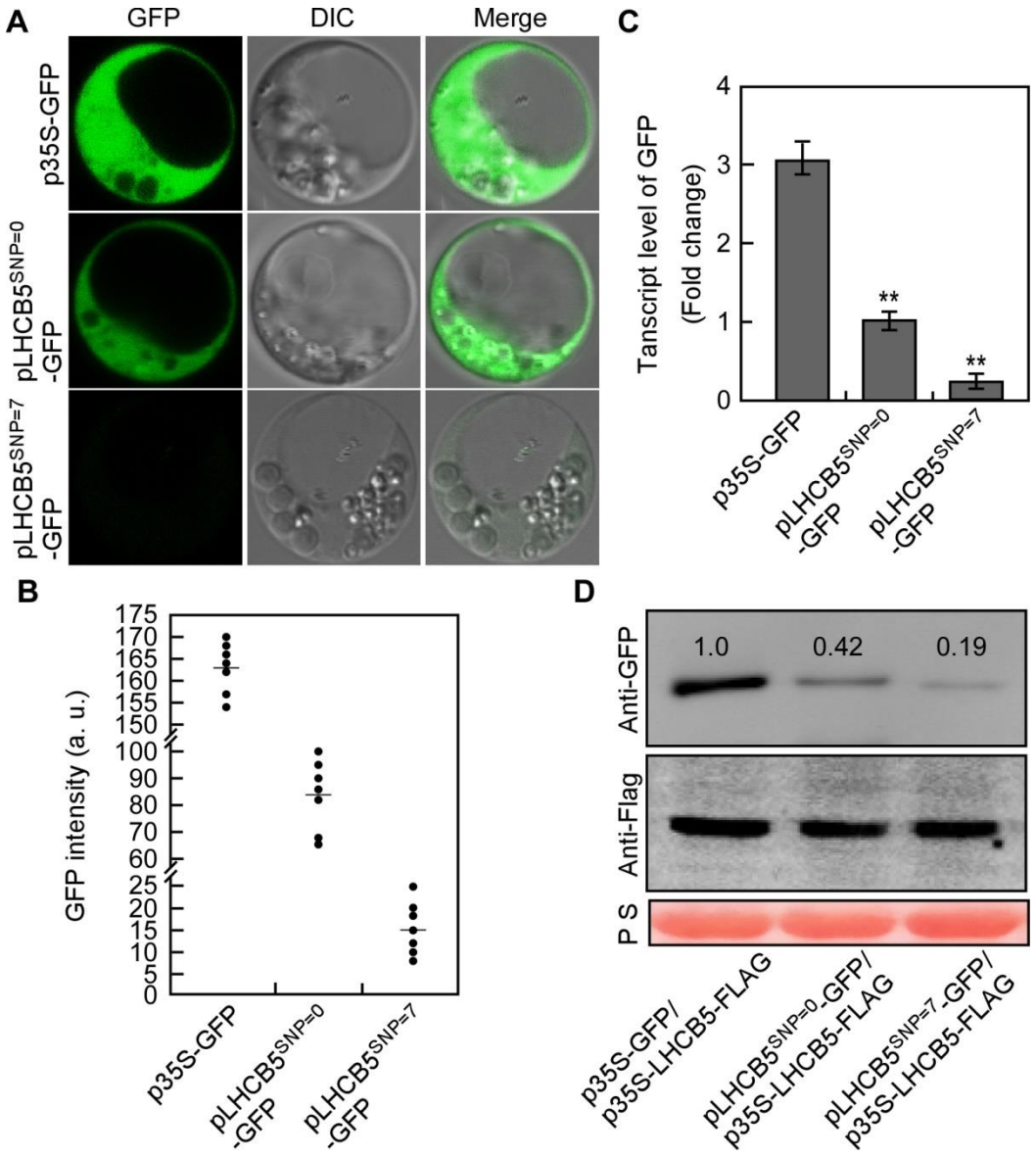

Fig. S7. SNP variations in promoter regulate gene transcription. (A and B) Transcript level assay of different SNP variations in the promoter of *LHCB5*. Rice protoplast of *LHCB5*-KO plants expressing GFP reporter gene driven by different promoters pBIN:p35S:GFP, pBIN:pLHCB5$^{SNP=0}$:GFP and pBIN:pLHCB5$^{SNP=7}$:GFP. The images were captured in a confocal microscope 16 h after transfection with the same level of exposure. **(C) The transcript level of *LHCB5* expressed by different promoters**. The expression level of GFP was analyzed by qRT-PCR (T-test, ***P*<0.01). **(D) Western blot assay for the protein level of GFP driven by different promoters.** Rice protoplast of *LHCB5*-KO plants expressing GFP reporter gene driven by different promoters pBIN:p35S:GFP, pBIN:pLHCB5$^{SNP=0}$:GFP and pBIN:pLHCB5$^{SNP=7}$:GFP (p35S:LHCB5:Flag was co-expressed to ensure the same transform efficiency). Protein loading is indicated with Ponceau staining (P S).

Figure S8

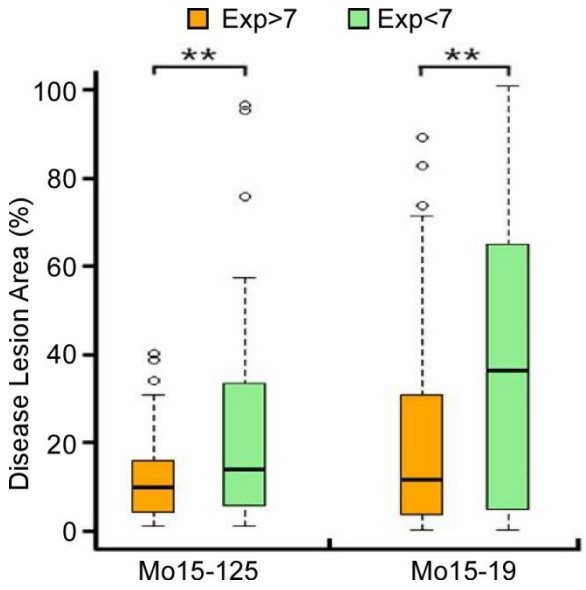

Fig. S8. LHCB5 resistance is associated with *LHCB5* transcript levels.

The resistance of 238 rice varieties mentioned above was correlated with the expression of *LHCB5*. The disease lesion area was present in Dataset S3. The yellow boxes indicate the expression level is greater than 7 and the green boxes indicate the expression level is below 7. Mo15-125 and Mo15-19 were *M. oryzae* isolates used for resistance assay. Values are the means of three replications, and error bars represent the SD (n = 3). The asterisks indicate a significant difference according to Student's t-test ($P < 0.01$).

Figure S9

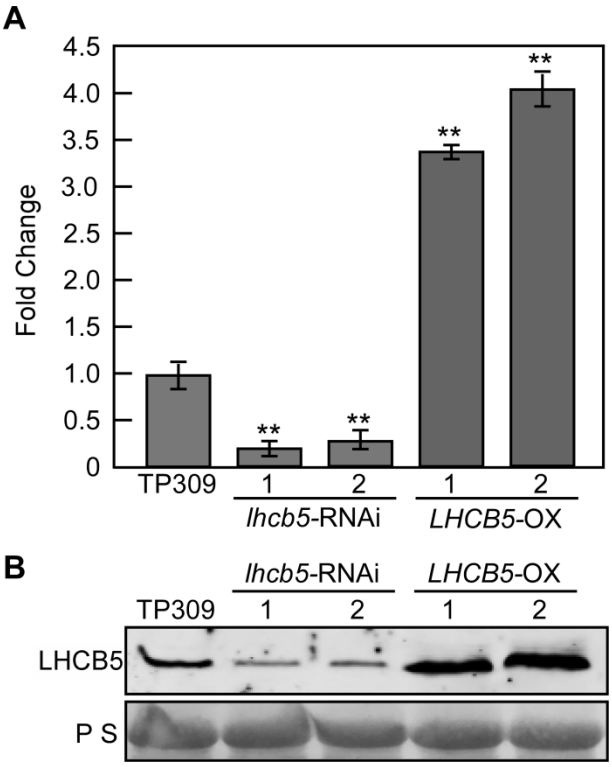

Fig. S9. The verification of transgenic plants.

(A) The transcript level of *LHCB5* in the transgenic plants. The expression level of *LHCB5* in the overexpression (*LHCB5*-OX, pCAM2300-*LHCB5*-Flag) and RNAi (*lhcb5*-RNAi, pUCCRNAi-*LHCB5*) plants was determined by qRT-PCR. The expression level of the *ACTIN* gene was used as an internal control. (Student's t-test, $^{**}P < 0.01$). **(B) Protein amount of LHCB5 in the transgenic plants.** The protein level of LHCB5 in the *LHCB5*-OX and *lhcb5*-RNAi plants was determined by immunoblotting. Total protein was extracted from rice seedlings and subjected to SDS-PAGE, followed by immunoblot analysis using an anti-LHCB5 polyclonal antibody. Protein loading is indicated with Ponceau staining (P S).

Figure S10

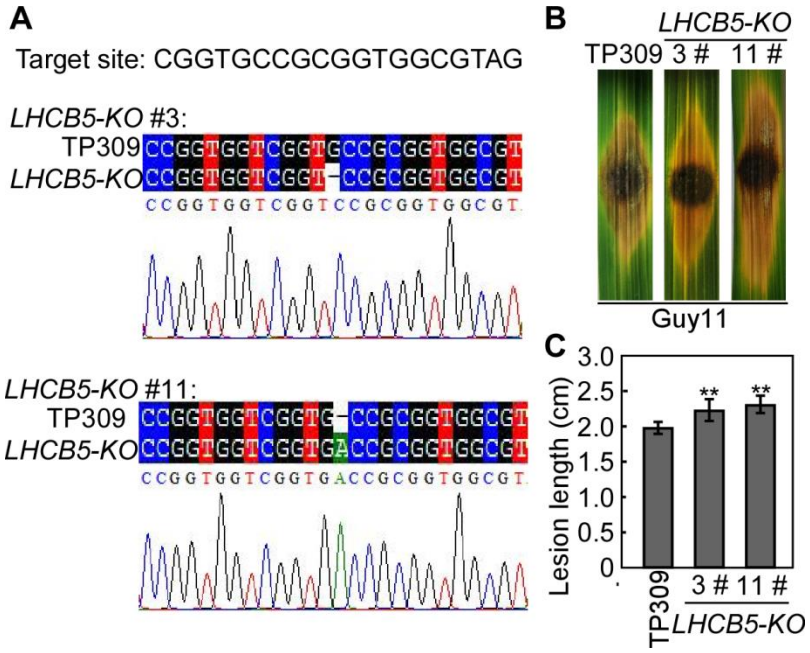

Fig. S10. Determination of the resistance of the *LHCB5* knockout transgenic lines. (A) Target site designed and verification for knocking out the *LHCB5* gene by CRISPR/Cas9 system. The *LHCB5*-KO lines were verified by PCR-based sequencing. Two representative transgenic lines (*LHCB5*-KO #3 and *LHCB5*-KO #11) are generated from TP309 genetic background. **(B) Infection phenotype of *LHCB5*-KO lines.** The leaves of 4-week-old plants were infected with Guy11 using punch inoculation. Photos were taken at 6 dpi. **(C)** Lesion length was measured 6 dpi. Values are the means of three replications, and error bars represent the SD (n = 3). The asterisks indicate a significant difference according to Student's t-test ($P < 0.01$).

Figure S11

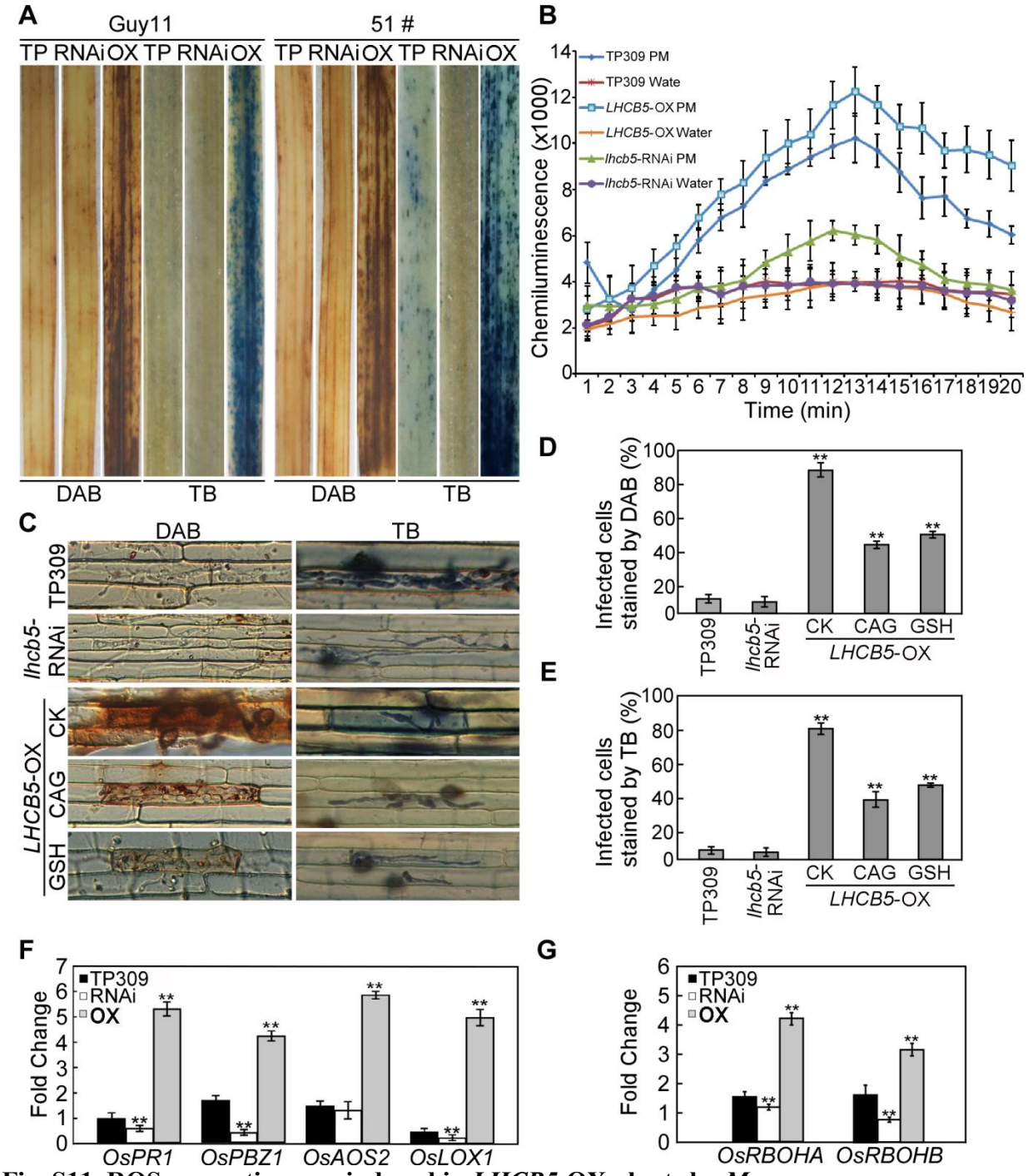

Fig. S11. ROS generation was induced in *LHCB5*-OX plants by *M. oryzae*.

(A) DAB and Trypan blue (TB) staining on infected leaves of TP309, *lhcb5*-RNAi and *LHCB5*-OX plants 2 days post inoculated with compatible strain Guy11 and incompatible strain 51 #. (B) Measurement of PM induced ROS burst. Leaf disks from the TP309, *lhcb5*-RNAi, and *LHCB5*-OX plants were treated with 100 nM PM and water. ROS were detected with a luminol-chemiluminescent assay. Error bars represent the SD (n = 3). (C) DAB and TB staining on infected leaf sheath of TP309, *lhcb5*-RNAi, and *LHCB5*-OX plants. (D and E) Statistics of

infected cells stained with DAB and TB. Invasive growth of IH restored by CAG and GSH treatment. 100 penetration sites of each sample were counted. (F and G) Induction of the defense-related genes (*OsPR1*, *OsPBZ1*, *OsAOS2,* and *OsLOX1*) and NADPH oxidase (*RBOHA* and *RBOHB*) in *LHCB5*-OX plants inoculated with Guy11. qPCR was performed with gene-specific primers. Values are the means of three replications, and error bars represent the SD (n = 3). The asterisks indicate a significant difference according to Student's t-test ($P < 0.01$).

Figure S12

Pi gene / Isolate	Piks Pish	Pia Pi19	Pii Pish	Pik Pish	Pikm Pish	Piz Pish	Pita	Pita2 Pish	Pizt Pish	Pikp Pish	Pib Pish	Pit Piks	Pikh
Guy11	S	R	S	S	S	R	S	S	S	S	R	S	S
98-06	R	R	R	R	R	R	R	R	R	R	R	R	R
98-21-1	S	S	R	S	S	S	S	R	R	S	R	S	S
98-24-1	S	S	R	S	S	S	S	R	R	R	R	S	R
98-55-1	S	R	R	R	R	R	S	S	R	R	R	S	R
98-83-1	S	S	R	R	R	R	R	S	R	R	R	R	R
98-84-1	S	R	R	R	R	R	S	S	R	R	R	S	R
98-93-1	S	S	R	R	R	R	S	S	R	R	R	S	R
99-21	S	R	R	R	R	R	S	S	R	R	R	R	R
99-27	S	R	R	R	R	R	S	S	R	R	R	S	R
99-46	S	R	R	S	S	R	S	S	R	S	R	R	S
99-66-1	S	R	R	R	R	R	S	S	R	S	R	R	R
99-106-2	S	R	R	R	R	R	S	S	R	R	R	S	R
JS001-19	S	S	R	S	R	S	S	R	R	R	S	S	R
JS001-32	S	R	R	S	R	S	S	S	S	S	S	S	R
JS001-33	S	S	R	S	S	S	R	S	S	R	R	S	R
2002-10-2	S	R	S	R	S	R	S	S	R	R	R	R	R
8036-2	R	R	R	R	R	R	R	S	R	R	R	R	R
9403-3	R	R	R	R	R	R	R	S	R	R	R	R	R
2013-19	S	S	S	S	R	S	S	S	S	S	S	S	S
2013-46	S	R	S	R	R	S	S	R	R	R	S	S	R

Fig. S12. The resistance of different known blast *R* genes to 21 *M. oryzae* isolates collected from different rice growing regions in China.

Two-week-old seedlings were spray-inoculated with 21 blast isolates collected in China. Disease resistance was scored at 7 dpi. R: resistant, S: susceptible.

Figure S13

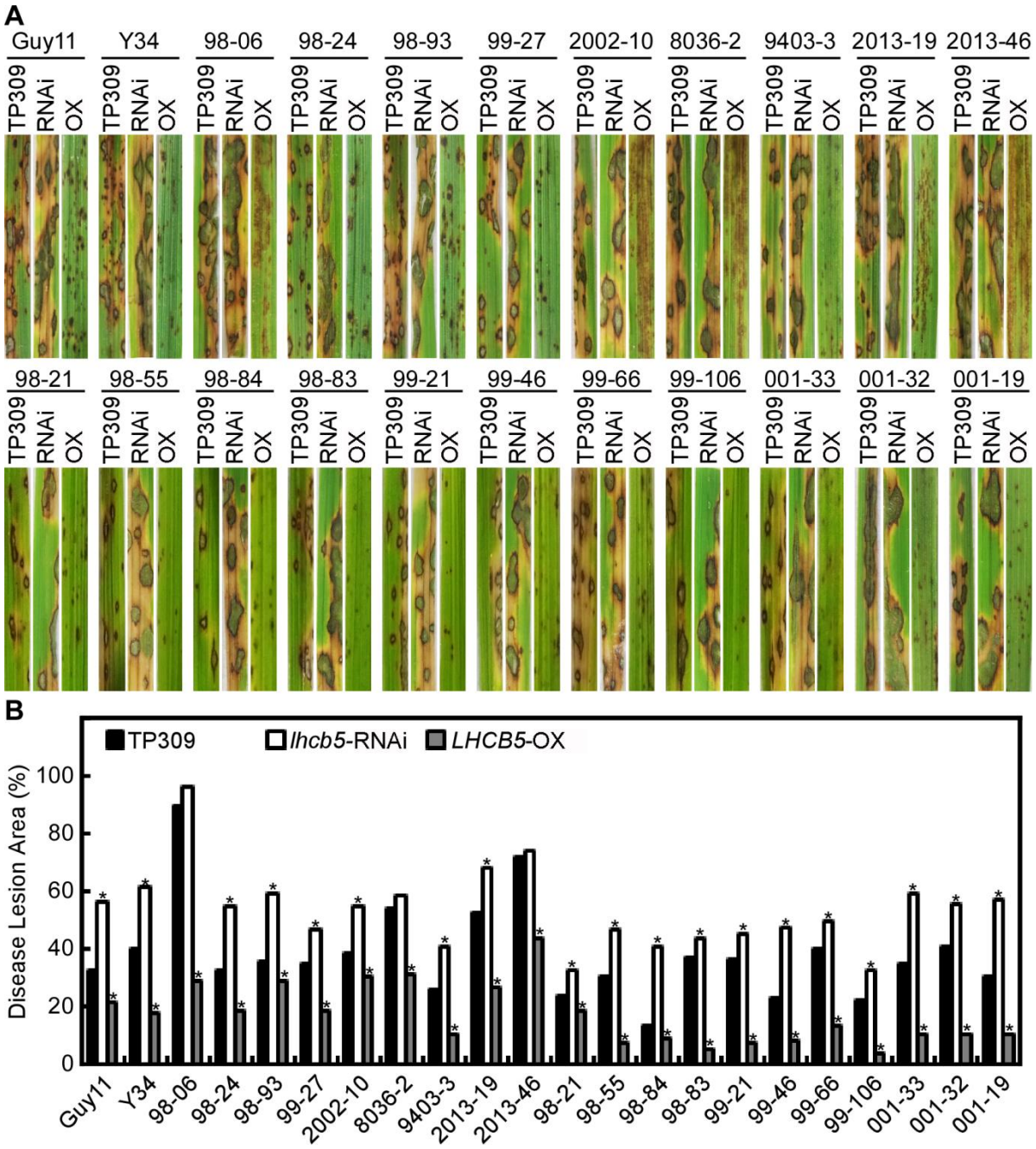

Fig. S13. Determination of the broad-spectrum blast resistance of the *LHCB5*-OX plant.

(A) **Blast resistance assay of the *LHCB5*-OX plant.** Blast resistance of TP309, *lhcb5*-RNAi and *LHCB5*-OX plants to 21 blast isolates showed in figure S9 using spraying inoculation. Photos were taken at 7 dpi. (B) **Disease lesion area (DLA) of the leaves infected by 21 blast isolates was measured by Image J**. Lesions were measured or scored at 7 dpi and experiments were repeated twice with similar results. Values are the means of three replications, and error bars represent the SD (n = 3). The asterisks indicate a significant difference according to Student's t-test ($P < 0.01$).

Figure S14

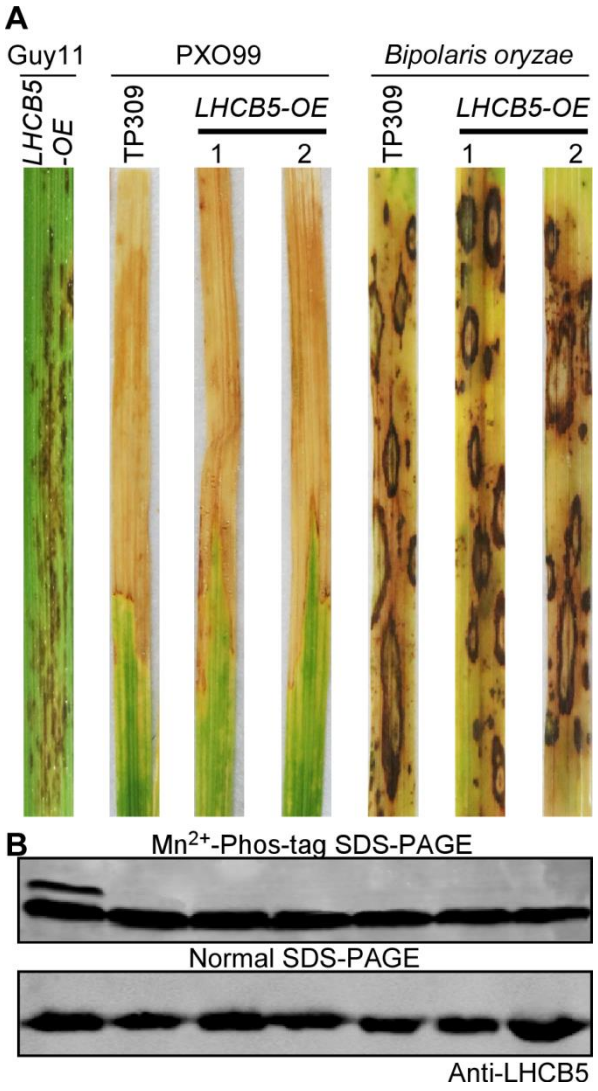

Fig. S14. Determination on *X. oryzae* and *B. oryzae* resistance of *LHCB5*-OX plants.

(A) *X. oryzae* and *B. oryzae* resistance assay of *LHCB5*-OX plants. The TP309 and *LHCB5*-OX plants were inoculated with *X. oryzae* using the bacterial fluid. The water-soaked lesions appeared on TP309 and *LHCB5*-OX plants. Pictures were taken at 12 dpi. The TP309 and *LHCB5*-OX plants were inoculated with *B. oryzae* using conidia. Pictures were taken at 6 dpi. **(B) LHCB5 was not phosphorylated in *LHCB5*-OX plants inoculated with *X. oryzae* and *B. oryzae*.** Proteins from TP309 and *LHCB5*-OX cell extracts treated with phosphatase inhibitors were subjected to Phos-tag SDS-PAGE and normal SDS-PAGE followed by immunoblotting with the LHCB5 polyclonal antibody.

Figure S15

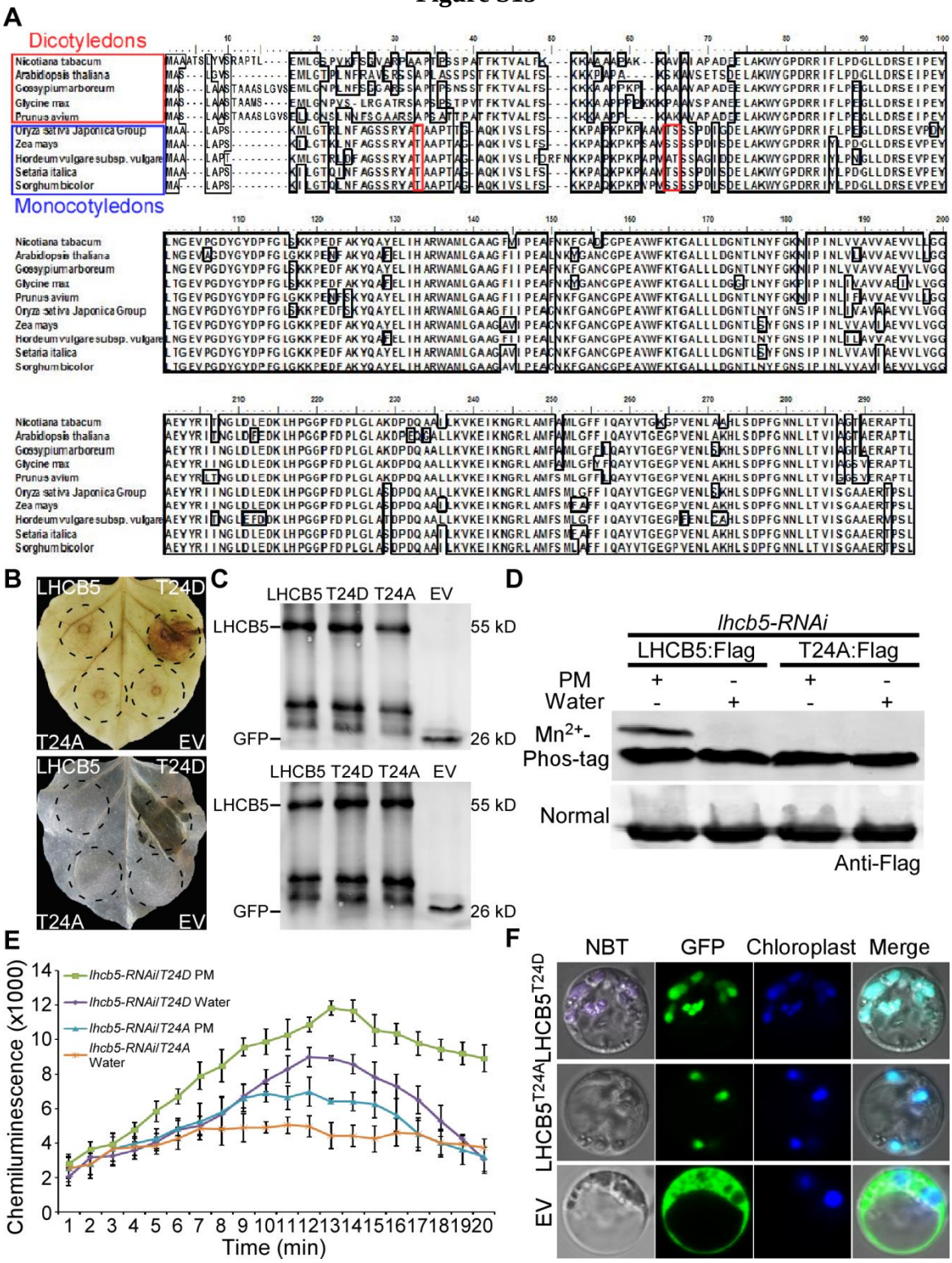

Fig. S15. Phosphorylation of LHCB5 24th threonine.

(A) Sequence alignment of LHCB5 proteins from dicotyledon and monocotyledon plants. Red boxes indicated three conserve phosphorylation sites in LHCB5 predicted by DISPHOS 1.3 and NetPhos 3.1 server. **(B) Constitutively activated the 24th threonine of OsLHCB5**

induced ROS production in *N. benthamiana*. Leaves were infiltrated with A. tumefaciens cells containing PVX:GFP (EV) vector and PVX vector carrying the rice LHCB5 gene, constitutively activated form (PVX:LHCB5^{T24D}:GFP), or constitutively inactivated form (PVX:LHCB5^{T24A}:GFP). Images were taken at 5 d after infiltration. The left leaf was stained by DAB and the right leaf was decolorized with ethanol. **(C)** Immunoblot analysis of proteins from N. benthamiana leaves transiently expressing LHCB5, LHCB5^{T24D} and LHCB5^{T24A} fused with GFP tag. The protein extracts were subjected to normal SDS-PAGE followed by immunoblotting with the anti-GFP antibody. **(D)** Detection of phosphorylation in rice protoplasts. Rice protoplasts of *lhcb5*-RNAi plants expressing LHCB5:Flag and LHCB5^{T24A}:Flag were induced with PM or water. The protein extracts were subjected to Phos-tag SDS-PAGE and normal SDS-PAGE followed by immunoblotting with anti-Flag antibody. **(E)** Measurement of the ROS burst in *lhcb5*-RNAi plants expressed pBIN:LHCB5^{T24D}:GFP and pBIN:LHCB5^{T24A}:GFP using a luminol-chemiluminescence assay. **(F)** Rice protoplast of *lhcb5*-RNAi plants expressing pBIN:GFP (EV), pBIN:LHCB5^{T24D}:GFP and pBIN:LHCB5^{T24A}:GFP were stained by nitroblue tetrazolium (NBT). The images were captured with a confocal microscope 16 hr after transfection. Chloroplasts are autofluorescence in blue.

Figure S16

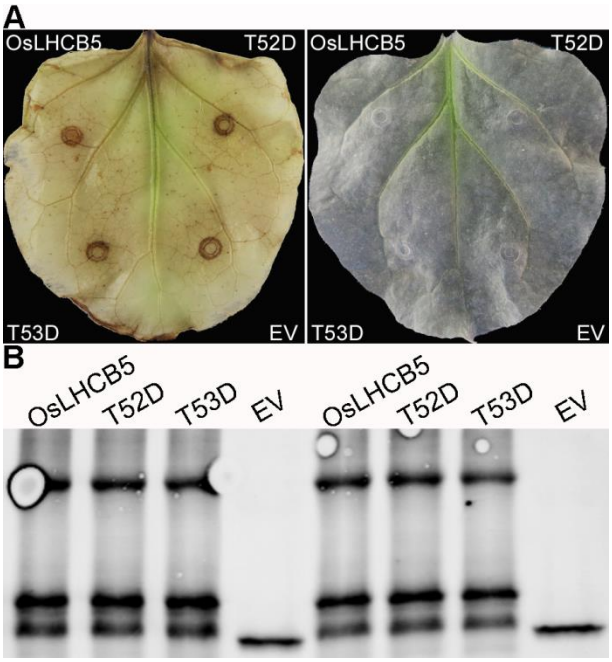

Fig. S16. Constitutively activated the Thr52 and Ser53 of LHCB5 can't induce ROS production in *N. benthamiana*.

(A) **Function analysis of the 52nd threonine 53rd serine of LHCB5.** *N. benthamiana* leaves were infiltrated with *A. tumefaciens* cells containing PVX:GFP (EV) vector and PVX vector carrying the *LHCB5* gene, constitutively activated form PVX:LHCB5^{T52D}:GFP and PVX:LHCB5^{S53D}:GFP. Photos were taken at 5 days after infiltration. The left leaf was stained with DAB. Both leaves were decolorization with ethanol. (B) **Immunoblot analysis of proteins from *N. benthamiana* leaves transiently expressing LHCB5, LHCB5^{T52D} and LHCB5^{S53D} fused with the GFP tag.**

Figure S17

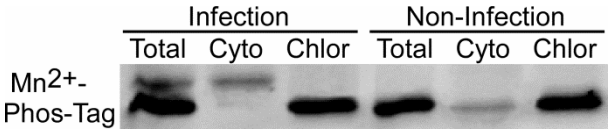

Fig. S17. LHCB5 is phosphorylated in the cytoplasm.

The total, chloroplast and cytoplasm proteins of *LHCB5*-OX plants inoculated with or without Guy11 were extracted and subjected to Phos-tag SDS-PAGE followed by immunoblotting with the LHCB5 polyclonal antibody.

Figure S18

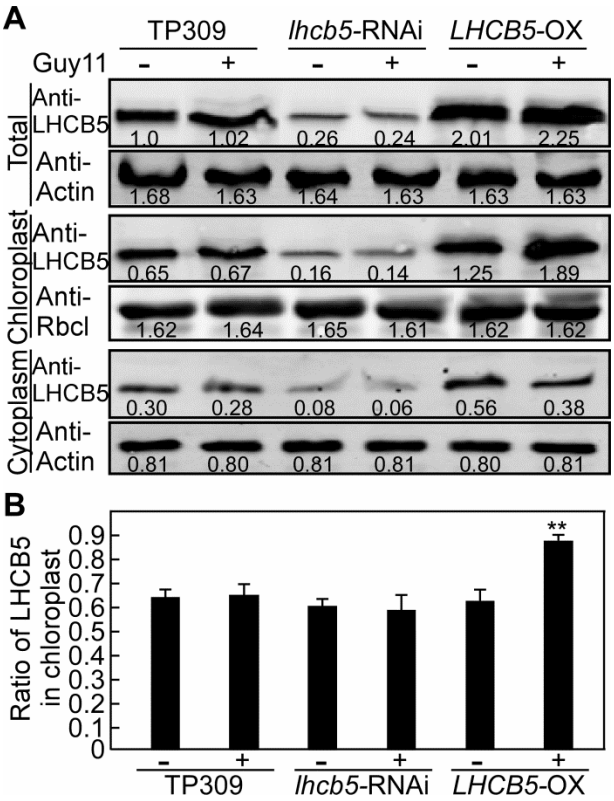

Fig. S18. The accumulation of LHCB5 in the chloroplast.

(A) **The protein amount of LHCB5 in the chloroplast.** The total, chloroplast and cytoplasm proteins of TP309, *lhcb5*-RNAi and *LHCB5*-OX plants inoculated with or without Guy11 were extracted (equally amount of rice leaves) and subjected to SDS-PAGE followed by immunoblotting with an LHCB5 polyclonal antibody. The chloroplast protein is immunoblotted with the Rbcl polyclonal antibody. The total and chloroplast proteins are immunoblotted with the actin polyclonal antibody. (B) **The ratio of LHCB5 in the chloroplast.** The relative band intensity was quantified by ImageJ software.

Figure S19

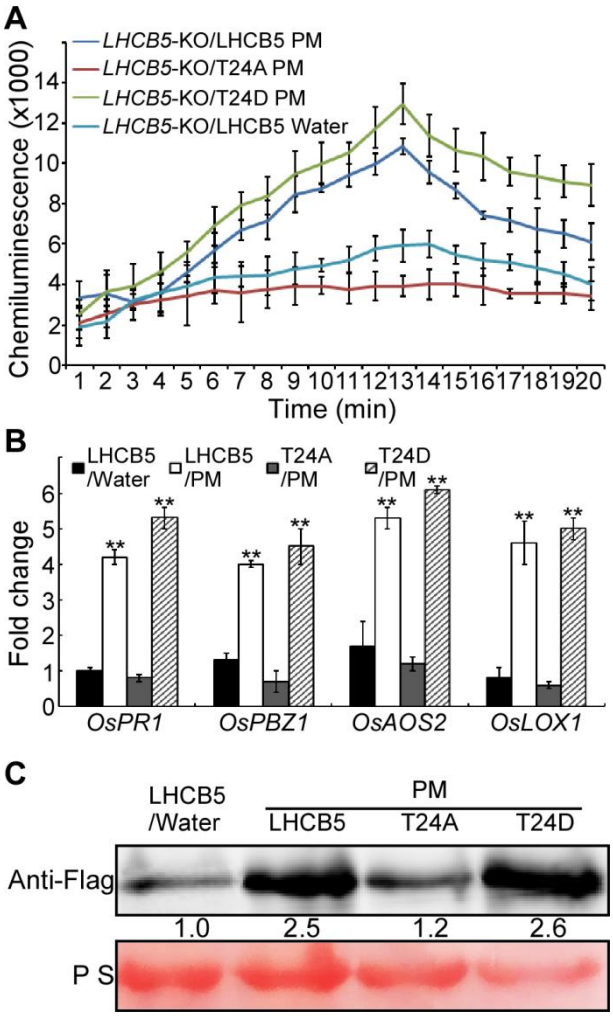

Fig. S19. Phosphorylation of LHCB5 24th threonine determines the protein accumulation in chloroplast and immune response. (A) Measurement of the ROS burst in *LHCB5*-KO plants. The protoplast of *LHCB5*-KO plants expressed pBIN:LHCB5:Flag, pBIN:LHCB5^{T24A}:Flag and pBIN:LHCB5^{T24D}:Flag treated with PM or water using a luminol-chemiluminescence assay. **(B) Phosphorylation of LHCB5 24th threonine induced the expression of defense-related genes.** qPCR was performed with gene-specific primers. Values are the means of three replications, and error bars represent the SD (n = 3). The asterisks indicate a significant difference according to Student's t-test ($P < 0.01$). **(C) Phosphorylation of LHCB5 24th threonine facilitates LHCB5 accumulation in the chloroplast**. The chloroplast proteins in protoplast of *LHCB5*-KO plants expressed pBIN:LHCB5:Flag, pBIN:LHCB5^{T24A}:Flag and pBIN:LHCB5^{T24D}:Flag treated with PM or water were extracted and subjected to SDS-PAGE followed by immunoblotting with the anti-Flag antibody. Protein loading is indicated with Ponceau staining (P S).

Figure S20

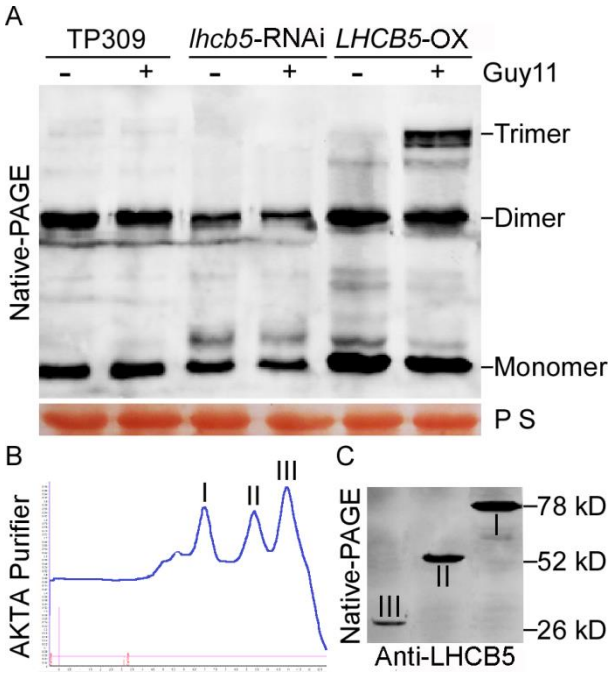

Fig. S20. Trimerization of LHCB5 in *LHCB5*-OX plants induced by *M. oryzae*.

(A) Immunoblot analysis of proteins isolated from TP309, *lhcb5*-RNAi and *LHCB5*-OX plants inoculated with or without Guy11. The total proteins of TP309, *lhcb5*-RNAi and *LHCB5*-OX plants inoculated with or without Guy11 were extracted and subjected to Native-PAGE followed by immunoblotting with LHCB5 polyclonal antibody. Protein loading is indicated with Ponceau staining (P S). **(B) Protein purification of LHCB5 *in vitro*.** The LHCB5 protein expressed *in vitro* using pET32a vector and separated by the AKTA protein purification system (GE healthcare). Three protein peaks were detected (I, II and III). **(C) Immunoblot analysis of proteins isolated from (B).** The separated proteins (I, II and III) were subjected to native-PAGE followed by immunoblotting with the LHCB5 polyclonal antibody.

Figure S21

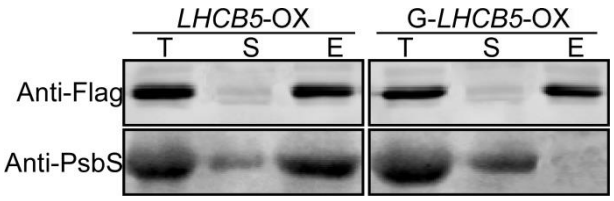

Fig. S21. The interaction between LHCB5 and PsbS.

Total proteins were extracted from *LHCB5*-OX (pCAM2300-LHCB5-Flag) leaves inoculated with or without Guy11 for *in vivo* Co-IP of LHCB5 and PsbS. The immune complexes were pulled down using anti-Flag agarose beads and then subjected to SDS-PAGE followed by immunoblotting with anti-Flag antibody and PsbS polyclonal antibody. “T” means Total protein, “S” means Supernatant, “E” means Elusion.

Figure S22

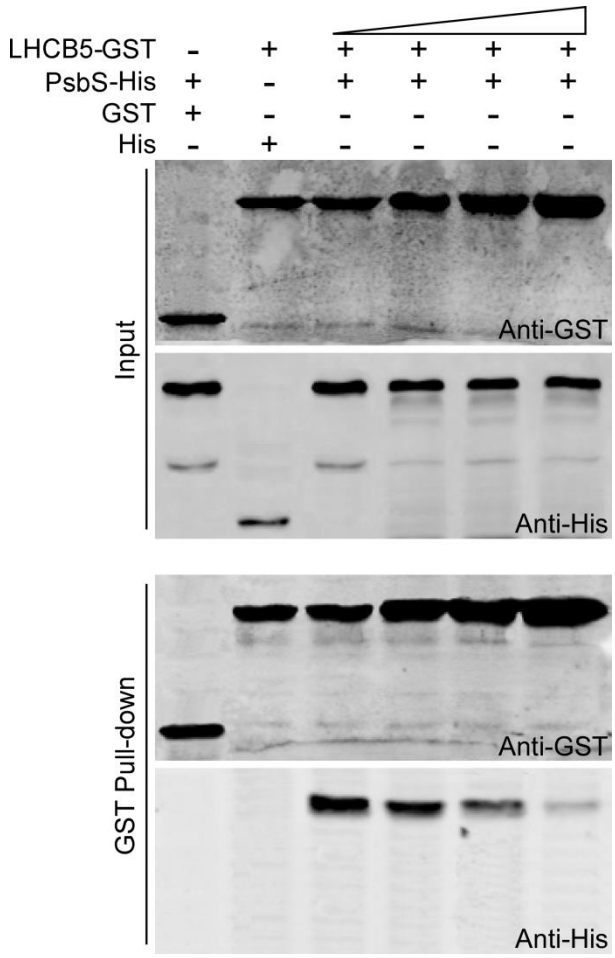

Fig. S22. Trimerization of LHCB5 affects the binding of PsbS.

LHCB5:GST (pGEX4T-2:LHCB5:GST) and PsbS:His (pET32a:PSBS:HIS) were expressed in *E.coli* stain BL21, the fused proteins were examined by Western blotting before (input) and after affinity purification (GST pull-down). Different gradient dilutions (1x, 2x, 3x, and 4x) of LHCB5:GST were added to the mix. The immune complexes were pulled down using anti-GST agarose beads and then subjected to SDS-PAGE followed by immunoblotting with the anti-GST and anti-HIS antibodies.

Figure S23

A

Lines	Chl a/b	Fv/Fm	ϕPSII	ETR
TP309	2.401 ± 0.05 a	0.823 ± 0.04 a	0.631 ± 0.07 a	54.391 ± 4.69 a
lhcb5-RNAi	2.486 ± 0.05 a	0.821 ± 0.05 a	0.658 ± 0.03 a	53.800 ± 4.26 a
LHCB5-OX	2.520 ± 0.07 a	0.848 ± 0.07 a	0.640 ± 0.04 a	54.910 ± 3.26 a
G-TP309	2.396 ± 0.07 a	0.819 ± 0.07 a	0.622 ± 0.04 a	51.829 ± 5.68 b
G-*lhcb5*-RNAi	2.481 ± 0.03 a	0.811 ± 0.03 a	0.633 ± 0.03 a	50.723 ± 1.79 b
G-*LHCB5*-OX	2.503 ± 0.02 a	0.803 ± 0.04 a	0.625 ± 0.08 a	40.882 ± 1.27 c

B

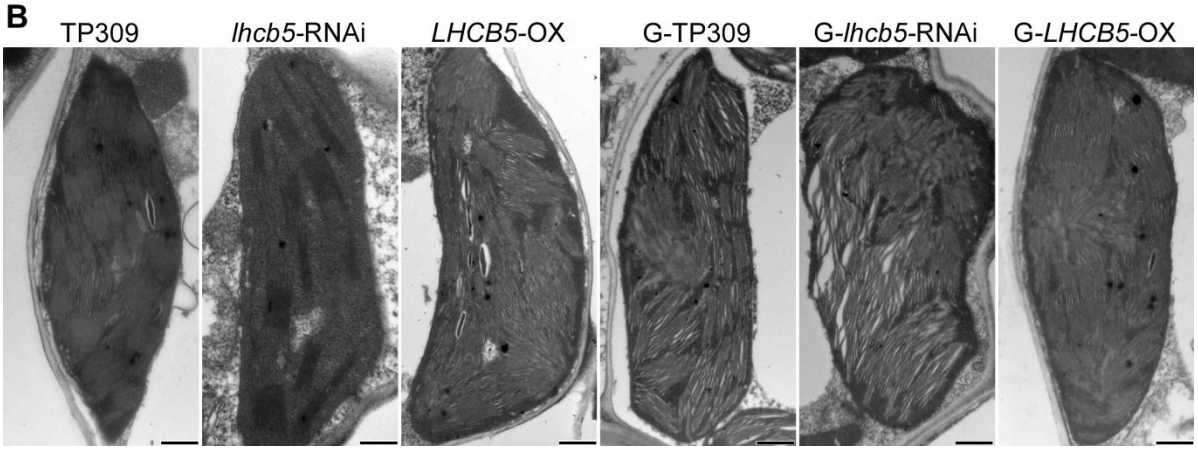

Fig. S23. Determination of photosynthetic parameters and chloroplast morphology in transgenic plants.

(A) Photosynthetic parameters in transgenic plants. The photosynthetic parameters of two-week-old rice leaves of TP309, G-TP309 (Guy11 infected), *lhcb5*-RNAi, G-*lhcb5*-RNAi (Guy11 infected), *LHCB5*-OX and G-*LHCB5*-OX (Guy11 infected) were determined by Chlorophyll Fluorescence Imager (Ecotek, Beijing). (B) **Transmission electron microscope analysis of chloroplast morphology in transgenic plants inoculated with or without Guy11.** Bar=500 nm.

Figure S24

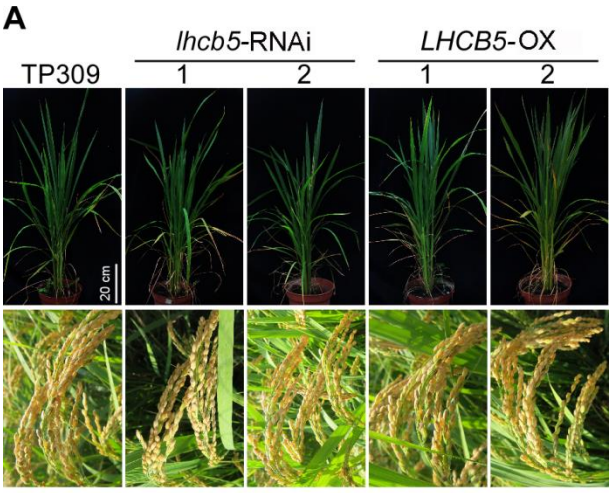

B

Lines	Height (cm)	TGW (g)	SSR (%)
TP309	98.16 ± 1.3	26.11 ± 0.1	67.5 ± 1
Ihcb5-RNAi-1	97.81 ± 1.2	26.06 ± 0.3	66.9 ± 1.2
Ihcb5-RNAi-2	95.93 ± 1.6	26.10 ± 0.1	67.6 ± 1
LHCB5-OX-1	97.69 ± 1.2	26.09 ± 0.1	68.0 ± 1.5
LHCB5-OX-2	98.32 ± 1.3	26.13 ± 0.2	67.4 ± 1

Fig. S24. The phenotype of *LHCB5* transgenic plants.

(A) The photos showed 6-weeks-old transgenic plant growth in the field and the seed yield phenotype. (B) The height, thousand-grain weights (TGW) and seed setting rate (SSR) were measured after rice paddy matured.

Figure S25

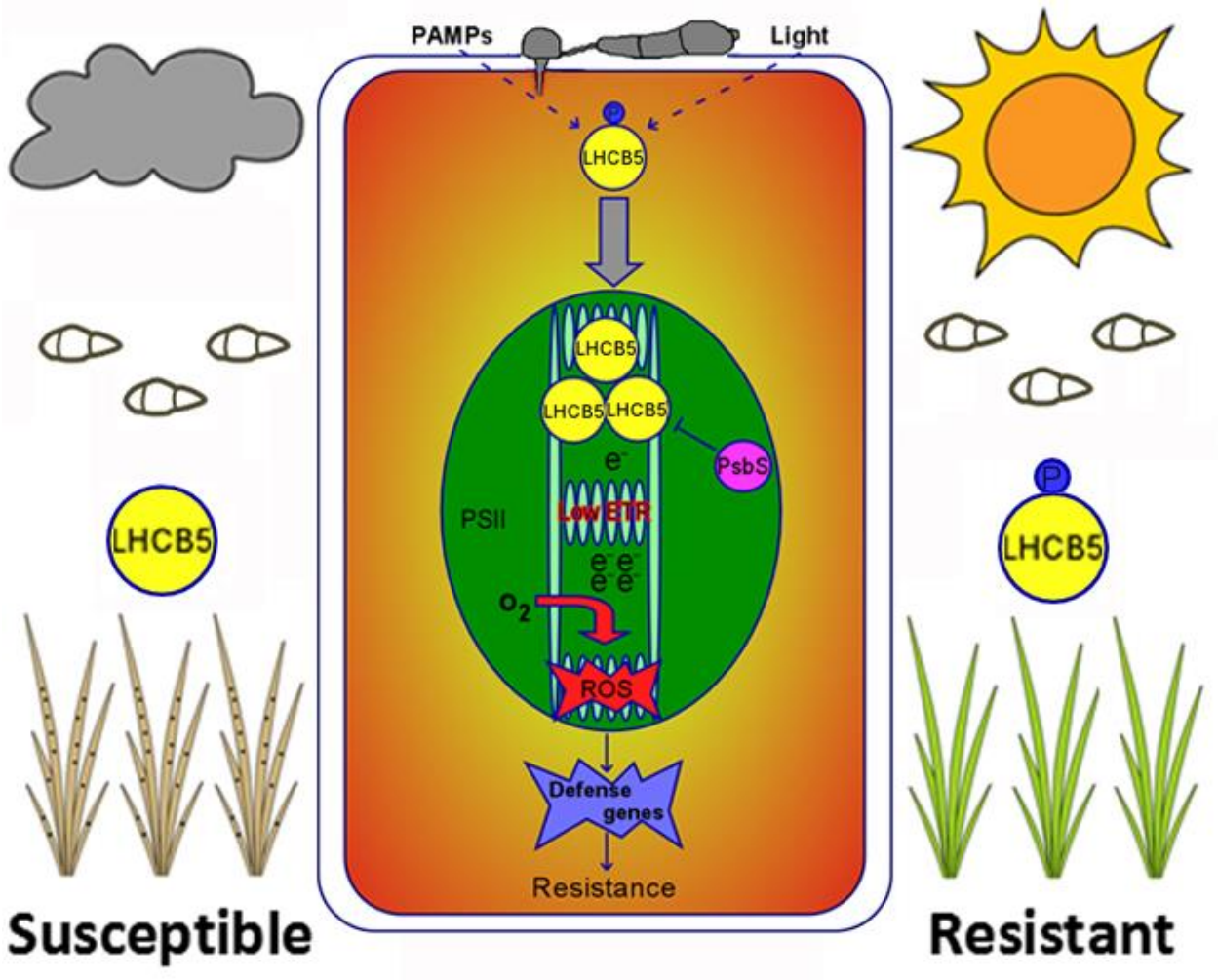

Fig. S25. The working model of LHCB5 regulated resistance in rice.

During the interaction of rice-*M. oryzae*, rice monitors the infection of the blast through the phosphorylation of LHCB5 in a light-dependent manner. Once the rice recognized the signals released by the blast, the kinase pathway will be activated, leading to the phosphorylation of LHCB5. The activated LHCB5 accelerated its accumulation in the chloroplast, resulting in trimerization, which helps to maintain the chloroplast morphology and affects its binding of PsbS and reduction in ETR. The accumulated electron reacts with oxygen to form ROS that functions as a signal to activate defense response thereby inducing resistance.

References

1. D. Fu, et al. (2009) A kinase-START gene confers temperature-dependent resistance to wheat stripe rust. *Science* 323, 1357.
2. C. Cheng, et al. (2013) Plant immune response to pathogens differs with changing temperatures. *Nat Commun* 4, 2530.
3. X. F. Xin, et al. (2016) Bacteria establish an aqueous living space in plants crucial for virulence. *Nature* 539, 524.
4. Y. Ren, P. Gao, F. Zhu (2016) Meteorological grade prediction of occurrence degree of rice blast in Jiangsu. *Jiangsu Agr Sci* 44, 151.
5. H. Zhang, X. Zheng, Z. Zhang (2016) The *Magnaporthe grisea* species complex and plant pathogenesis. *Mol Plant Pathol* 17, 796.
6. D. A. Dempsey, A. C. Vlot, M. C. Wildermuth, D. F. Klessig (2011) Salicylic acid biosynthesis and metabolism. *Arabidopsis Book* 9, e0156.
7. S. Fonseca, et al. (2009) (+)-7-iso-Jasmonoyl-L-isoleucine is the endogenous bioactive jasmonate. *Nat Chem Biol* 5, 344.
8. M. A. Strawn, et al. (2007) *Arabidopsis* isochorismate synthase functional in pathogen-induced salicylate biosynthesis exhibits properties consistent with a role in diverse stress responses. *J Biol Chem* 282, 5919.
9. A. Shapiguzov, J. P. Vainonen, M. Wrzaczek, J. Kangasjarvi (2012) ROS-talk - how the apoplast, the chloroplast, and the nucleus get the message through. *Front Plant Sci* 3, 292.
10. P. Pospisil (2012) Molecular mechanisms of production and scavenging of reactive oxygen species by photosystem II. *Biochim Biophys Acta* 1817, 218.
11. B. Hankamer, et al. (1997) Isolation and biochemical characterisation of monomeric and dimeric photosystem II complexes from spinach and their relevance to the organisation of photosystem II in vivo. *Eur J Biochem* 243, 422.
12. E. J. Boekema, J. F. van Breemen, H. van Roon, J. P. Dekker (2000) Arrangement of photosystem II supercomplexes in crystalline macrodomains within the thylakoid membrane of green plant chloroplasts. *J Mol Biol* 301, 1123.
13. J. Andersson, R. G. Walters, P. Horton, S. Jansson (2001) Antisense inhibition of the photosynthetic antenna proteins CP29 and CP26: implications for the mechanism of protective energy dissipation. *Plant Cell* 13, 1193.
14. S. de Bianchi, L. Dall'Osto, G. Tognon, T. Morosinotto, R. Bassi (2008) Minor antenna proteins CP24 and CP26 affect the interactions between photosystem II subunits and the electron transport rate in grana membranes of *Arabidopsis*. *Plant Cell* 20, 1012.
15. A. V. Ruban, et al. (2003) Plants lacking the main light-harvesting complex retain photosystem II macro-organization. *Nature* 421, 648.
16. S. Jansson (1994) The light-harvesting chlorophyll a/b-binding proteins. *Biochim Biophys Acta* 1184, 1.
17. P. Horton, A. V. Ruban, R. G. Walters (1996) Regulation of light harvesting in green plants. *Annu Rev Plant Physiol Plant Mol Biol* 47, 655.
18. J. Y. Li, J. Wang, R. S. Zeigler (2014) The 3,000 rice genomes project: new opportunities and challenges for future rice research. *Gigascience* 3, 8.
19. Z. Qi, et al. (2016) The syntaxin protein (MoSyn8) mediates intracellular trafficking to regulate conidiogenesis and pathogenicity of rice blast fungus. *New Phytol* 209, 1655.
20. A. R. Ayers, J. Ebel, B. Valent, P. Albersheim (1976) Host-Pathogen Interactions: X. fractionation and biological activity of an elicitor isolated from the mycelial walls of phytophthora megasperma var. sojae. *Plant Physiol* 57, 760.
21. S. Tanabe, Y. Nishizawa, E. Minami (2009) Effects of catalase on the accumulation of H_2O_2 in rice cells inoculated with rice blast fungus, *Magnaporthe oryzae*. *Physiol Plant* 137, 148.
22. Li J, et al. (2005) Hydrogen peroxide regulates elicitor PB90-induced cell death and defense in non-heading Chinese cabbage. *Physiol Mol Plant Pathol* 67(3-5):220-230.
23. Q. H. Chen, Y. C. Wang, X. B. Zheng (2006) Genetic diversity of *Magnaporthe grisea* in china as revealed by DNA fingerprint haplotypes and pathotypes. *J Phytopathol* 154, 361.
24. S. Lemeille, et al. (2009) Analysis of the chloroplast protein kinase Stt7 during state transitions. *PLoS Biol* 7, e45.

25. N. Depege, S. Bellafiore, J. D. Rochaix (2003) Role of chloroplast protein kinase Stt7 in LHCII phosphorylation and state transition in *Chlamydomonas*. *Science* 299, 1572.
26. E. Kinoshita, E. Kinoshita-Kikuta, K. Takiyama, T. Koike (2006) Phosphate-binding tag, a new tool to visualize phosphorylated proteins. *Mol Cell Proteomics* 5, 749.
27. G. Lamberti, C. Drurey, J. Soll, S. Schwenkert (2011) The phosphorylation state of chloroplast transit peptides regulates preprotein import. *Plant Signal Behav* 6, 1918.
28. T. May, J. Soll (2000) 14-3-3 proteins form a guidance complex with chloroplast precursor proteins in plants. *Plant Cell* 12, 53.
29. I. S. Zulfugarov, et al. (2014) Production of superoxide from photosystem II in a rice (*Oryza sativa L.*) mutant lacking PsbS. *BMC Plant Biol* 14, 242.
30. I. S. Zulfugarov, et al. (2016) Enhanced resistance of PsbS-deficient rice (*Oryza sativa L.*) to fungal and bacterial pathogens. *J Plant Biol* 59, 616.
31. J. Sacharz, V. Giovagnetti, P. Ungerer, G. Mastroianni, A. V. Ruban (2017) The xanthophyll cycle affects reversible interactions between PsbS and light-harvesting complex II to control non-photochemical quenching. *Nat Plants* 3, 16225.
32. Y. Zhu, et al. (2000) Genetic diversity and disease control in rice. *Nature* 406, 718.
33. W. Bimolata, et al. (2015) Nucleotide diversity analysis of three major bacterial blight resistance genes in rice. *PLoS One* 10, e0120186.
34. M. A. Rashid, et al. (2016) Nucleotide diversity, natural variation, and evolution of flexible culm-1 and strong culm-2 lodging resistance genes in rice. *Genome* 59, 473.
35. W. Li, et al. (2017) A natural allele of a transcription factor in rice confers broad-spectrum Blast Resistance. *Cell* 170, 114.
36. J. Liao, et al. (2016) Pathogen effectors and plant immunity determine specialization of the blast fungus to rice subspecies. *Elife* 5, e19377.
37. J. Su, et al. (2018) Active photosynthetic inhibition mediated by MPK3/MPK6 is critical to effector-triggered immunity. *PLoS Biol* 16, e2004122.
38. S. Fukuoka, et al. (2009) Loss of function of a proline-containing protein confers durable disease resistance in rice. *Science* 325, 998.
39. B. Zhou, et al. (2006) The eight amino-acid differences within three leucine-rich repeats between Pi2 and Piz-t resistance proteins determine the resistance specificity to *Magnaporthe grisea*. Mol Plant-MicrobeInteract 19, 1216.
40. J. Huang, et al. (2014) Rapid evolution of avirulence genes in rice blast fungus *Magnaporthe oryzae*. *BMC Genet* 15, 45.
41. L. Li, et al. (2017) MoCAP proteins regulated by MoArk1-mediated phosphorylation coordinate endocytosis and actin dynamics to govern development and virulence of *Magnaporthe oryzae*. *PLoS Genet* 13(5):e1006814.
42. C. H. Park, et al. (2016) The E3 Ligase APIP10 Connects the Effector AvrPiz-t to the NLR Receptor Piz-t in Rice. *PLoS Pathog* 12(3):e1005529.
43. Y. Liu, et al. (2007) Chloroplast-generated reactive oxygen species are involved in hypersensitive response-like cell death mediated by a mitogen-activated protein kinase cascade. *Plant Journal* 51(6):941-954.
44. M. Yi, et al. (2009) The ER chaperone LHS1 is involved in asexual development and rice infection by the blast fungus *Magnaporthe oryzae*. *Plant Cell* 21(2):681-695.
45. X. Liu, et al. (2016) The Putative Protein Phosphatase MoYvh1 Functions Upstream of MoPdeH to Regulate the Development and Pathogenicity in *Magnaporthe oryzae*. *Mol Plant Microbe Interact* 29(6):496-507.
46. S. C. Lung SC, M. D. Smith, S. D. Chuong (2015) Isolation of Chloroplasts from Plant Protoplasts. *Cold Spring Harb Protoc* 2015(10):895-899.

Table S1. Primers used in this study.

Primers used for transgenic rice construction	
pCAM2300-*OSLHCB5*-F	5’-ACGCGTCGACATGGCGGCGCTCGCCCCGTCCAAG-3’
pCAM2300-*OSLHCB5*-R	5’- AACTGCAGCAGGCTGGGCGTCCTCTCGG-3’
pUCCRNAi-*OSLHCB5*-F1	5’-AACTGCAGCAACTACTTCGGCAACAGCA-3’
pUCCRNAi-*OSLHCB5*-R1	5’-GGACTAGTCCCGTTCTTGATCTCCTTCA-3’
pUCCRNAi-*OSLHCB5*-F2	5’-ACGCGTCGACCAACTACTTCGGCAACAGCA-3’
pUCCRNAi-*OSLHCB5*-R2	5’-AACTGCAGCCCGTTCTTGATCTCCTTCA-3’
Primers used for the proteins expression in *N.benthamiana* and rice protoplast	
pBin-*OsLHCB5*:*GFP*-F	5’-AGCTGTACAAGGGTACCCCCATGGCGGCGCTCGCCCCG-3’
pBin-*OsLHCB5*:*GFP*-R	5’-CATCTAGAGGATCCGTCGACCCCCAGGCTGGGCGTCCTCTCGG-3’
PVX-*OsLHCB5*: *FLAG*-F	5’-TCCCCCGGGATGGCGGCGCTCGCCCCG-3’
PVX-*OsLHCB5*:*FLAG* -R	5’-ACGCGTCGACCAGGCTGGGCGTCCTCTCGG-3’
PVX-*OsLHCB5*^{T24A}: *FLAG*-F	5’-TCCCCCGGGATGGCGGCGCTCGCCCCGTCCAAGATGCTCGGCAC CCGGCTCAACTTCGCCGGCTCCTCCCGCTACGCCGCCGCGGCAC-3’
PVX-*OsLHCB5*^{T24A}: *FLAG*-R	5’-ACGCGTCGACCAGGCTGGGCGTCCTCTCGG-3’
PVX-*OsLHCB5*^{T24D}: *FLAG*-F	5’-TCCCCCGGGATGGCGGCGCTCGCCCCGTCCAAGATGCTCGGCAC CCGGCTCAACTTCGCCGGCTCCTCCCGCTACGCCGACGCGGCAC-3’
PVX-*OsLHCB5*^{T24D}: *FLAG*-R	5’-ACGCGTCGACCAGGCTGGGCGTCCTCTCGG-3’
Primers used for GST-pull down	
pGEX4T-2-*OsLHCB5*-F	5’- CCGGAATTCATGGCGGCGCTCGCCCCGTCCAAG-3’
pGEX4T-2-*OsLHCB5*-R	5’-ACGCGTCTACCAGGCTGGGCGTCCTCTCGG -3’
pET32a- *OsPSBS*-F	5’-CGGAATTCATGGCGCAGTCGATGCTGG-3’
pET32a- *OsPSBS*-R	5’-CCCAAGCTTCTCTTCGTCGTCGTCGCTGAC-3’
Primers used for qRT-PCR	
Q-*OsACTIN*-F	5’-GCGTGGACAAAGTTTTCAACCG-3’
Q-*OsACTIN*-R	5’-TCTGGTACCCTCATCAGGCATC-3’
Q-*OsLHCB1.1*-F	5’-CTCCATGTTCGGCTTCTTCG-3’
Q-*OsLHCB1.1*-R	5’-AACCACTGCTAAGCTACGGT-3’
Q-*OsLHCB2*-F	5’-CTCCATGTTCGGCTTCTTCG-3’
Q-*OsLHCB2*-R	5’-CTCCATGTTCGGCTTCTTCG-3’
Q-*OsLHCB3*-F	5’-CTCCATGTTCGGCTTCTTCG-3’

Q-*OsLHCB3*-R	5’-CGAGCGATGGAGAGAGAGAG-3’
Q-*OsLHCB4*-F	5’-CCCGGAGAAGAGGCTGTAC-3’
Q-*OsLHCB4*-R	5’-TCGAAGATGGTGGTGTGGAG-3’
Q-*OsLHCB5*-F	5’-CAACTACTTCGGCAACAGCA-3’
Q-*OsLHCB5*-R	5’-CCCGTTCTTGATCTCCTTCA-3’
Q-*OsLHCB6*-F	5’-TCGCCATGCTCATCTTCTACT-3’
Q-*OsLHCB6*-R	5’-TAGCGATCAAACACGAAGCG-3’
Q-*OsPR1*-F	5’-TCTTCATCACCTGCAACTACTC-3’
Q-*OsPR1*-R	5’-ATTCATCGGATTTATTCTCACC-3’
Q-*OsPBZ1*-F	5’-CTACTATGGCATGCTCAAGAT-3’
Q-*OsPBZ1*-R	5’-ATAGAAAGGCACATAAACACAA-3’
Q-*OsAOS2*-F	5’-CAATACGTGTACTGGTCGAATGG-3’
Q-*OsAOS2*-R	5’-AAGGTGTCGTACCGGAGGAA-3’
Q-*OsLOX1*-F	5’-GCATCCCCAACAGCACATC-3’
Q-*OsLOX1*-R	5’-AATAAAGATTTGGGAGTGACATATTGG-3’
Q-*OsRBOHA*-F	5’-TGGGATAATGGCTGGGTTGT-3’
Q-*OsRBOHA*-R	5’-TGCAGCCCTTGTATTCCTCA-3’
Q-*OsRBOHB*-F	5’-GGTTCCGACGTAACAAGCTC-3’
Q-*OsRBOHB*-R	5’-AACAGGAACAGCGAGGTACA-3’

Table S2. Reagent or resources

REAGENT OR RESOURCES	SOURCE	IDENTIFIER
Chemicals, Peptides, and Recombinant Proteins		
PVX:GFP	This paper	N/A
PVX:LHCB5:GFP	This paper	N/A
pBIN:GFP	This paper	N/A
pBIN:LHCB5:GFP	This paper	N/A
pGEX4T-2:LHCB5:GST	This paper	N/A
pET32a:PSBS:HIS	This paper	N/A
PVX:LHCB5:GFP	This paper	N/A
PVX:LHCB5^{T24A}:GFP	This paper	N/A
PVX:LHCB5^{T24D}:GFP	This paper	N/A
PVX:LHCB5^{T52D}:GFP	This paper	N/A
PVX:LHCB5^{S53D}:GFP	This paper	N/A
BIN:LHCB5^{T24A}:GFP	This paper	N/A
BIN:LHCB5^{T24D}:GFP	This paper	N/A
pCAM2300-*LHCB5*	This paper	N/A
pUCCRNAi-*LHCB5*	This paper	N/A
pGEX4T-2:LHCB5:GST	This paper	N/A
pET32a:PSBS:HIS	This paper	N/A
Critical Commercial Assays		
Luminol	Sigma-Aldrich	CAS#521-31-3
Peroxidase from horseradish	Sigma-Aldrich	CAS#9003-99-0
LHCB1 Antibody	Agrisera	AS01004
LHCB2 Antibody	Agrisera	AS01003
LHCB3 Antibody	Agrisera	AS01002
LHCB4 Antibody	Agrisera	AS01045
LHCB5 Antibody	Agrisera	AS01009
LHCB6 Antibody	Agrisera	AS01010
Experimental Models: Organisms/Strains		
Escherichia coli BL21	Takara	D90120-9125
A. tumefaciens GV3101	This paper	N/A

Additional Datasets S1-S3

Dataset S1. List of SNPs in the promoter and the coding sequences of *LHCB5* from 3,000 sequenced rice genomes.

Dataset S2. List of SNPs grouping in the promoter sequence of *LHCB5*.

Dataset S3. List of SNPs, transcription levels of *LHCB5* and blast resistance in 238 rice varieties.